IEEE Access
Multidisciplinary | Rapid Review | Open Access Journal

Received September 21, 2020, accepted October 4, 2020, date of publication October 6, 2020, date of current version October 21, 2020.

Digital Object Identifier 10.1109/ACCESS.2020.3029192

Unknown Radar Waveform Recognition Based on Transferred Deep Learning

ANNI LIN, ZHIYUAN MA, ZHI HUANG, YAN XIA, AND WENTING YU
Department of Electronic Technology, Naval University of Engineering, Wuhan 430033, China
Corresponding author: Zhiyuan Ma (mazhiyuan@mails.ccnu.edu.cn)

ABSTRACT Radar signals are emerging constantly for urgent task because of its complex patterns and rich working modes. For some radar waveforms with known modulation methods, they can be identified by correlation between radar prior knowledge and the received signals by the reconnaissance receiver. As for the unknown radar signals, how to identify unknown radar waveforms under the condition of limited samples and low signal-to-noise ratio is a challenging problem. Aiming at the learning ability of the deep features of the image by the convolutional neural network (CNN), the reconstructed features of the time-frequency image (TFI) of the known and unknown radar waveform signals have been excavated. A decision fusion unknown radar signal identification model based on transfer deep learning and linear weight decision fusion is designed in this paper. Firstly, the CNN is trained using the known radar signals; Then, based on the transfer learning, the neurons obtained from the multiple underlying the CNN are used to represent the reconstruction feature; Finally, the performance of the single random forest classifier of the original TFI and short- time autocorrelation features images (SAFI)are fused, the identification decision of unknown signals is realized by setting linear weight to the two databases. The recognition rate of unknown new classes for small samples exceeds 80.31%, and the classification accuracy rate for known radar waveform reach more than 99.15%.

INDEX TERMS Unknown radar waveform recognition, convolutional neural network, decision fusion, transfer learning, random forest.

I. INTRODUCTION

In modern electronic countermeasures, the analysis and processing of radar waveform is one of the important links of Electronic Intelligence Reconnaissance System (ELINT) and Electronic Support system (ESM) [1]. The radar signal styles are complicated and have many working modes. Especially in wartime, new radar signals continue to emerge for urgent task. For some radar waveforms with known modulation methods, they can be identified correlation between the prior knowledge and the radar signal received from the reconnaissance receiver. However, in the actual confrontation environment, both sides will use complex advanced technologies such as active phased array, frequency agility, multi-function and three-coordinate radar to generate unknown or new radar waveforms to circumvent the other's identification system. Because of its frequent update to follow the changing battlefield dynamics, the inappropriate rejection or identification of unknown radar emitter signals will cause an increase in false alarm (or missed alarm) rate, which directly affects the performance of electronic reconnaissance equipment and then affects predominating initiative in combat. In addition, the collected misjudgment signal data will mislead the platform in expanding the training database, decrease the reliability of classification model and cause secondary misleading to the battlefield personnel's judgment of subsequent signals. The challenging problem of how to identify unknown radar waveforms in the conditions of small-capacity samples, unlabeled samples and under low signal-to-noise ratio (SNR) has attracted more and more attention [2].

The sorting of unknown signals is mainly considered from two ways, the recognition mechanism and modeling. Similar to known radar waveform classifiers, feature extraction and classifier design are two key factors when the model is established. In the field of traditional radar waveform recognition, the radar pulse parameter-sequence is obtained by the frequency domain wide open receiving method. The pulse description word (PDW) can be gotten as the fingerprint feature of the radar signal, which is mainly composed of direction of arrival (DOA), carrier frequency (RF), pulse width (PW), pulse repetition interval (PRI) and pulse amplitude (PA). Literature [3] established two processing modes

The associate editor coordinating the review of this manuscript and approving it for publication was Jinming Wen.

for the recognition and training of unknown radar waveforms, and used expert knowledge and production rules to make logical judgments on PDW of unknown radar waveform. The average sorting rate of radar source signals for seven working conditions is 88%. Literature [4] selected RF, DOA, PA and pulse number as the multi-dimensional feature parameters, then the clustering method based on the Kohonen network model was used for the radar to pattern matching, and three types of radar waveform were sorted at the recognition rates of 94.1%, 100% and 94.2% respectively. Literature [5] optimized the k-means clustering method based on the network distance, the average sorting rate of five types of radar waveform reaches 92.3% under the interference of random noise. However, radar signal recognition based on PDW needs to separate independent pulses from randomly overlapping pulse streams. There was an excessive manual intervention in signal preprocessing. In addition, in a real electromagnetic environment, due to the high density of electromagnetic signals, in order to identify a large number of radar emitter signals, it is necessary to seek high-precision and stable parameter characteristic information of radar waveform.

For in-pulse feature, as the modulation method changes, it can reflect the comprehensive characteristics of the amplitude, frequency and phase of the signal. For the rich coverage of feature parameters and less parameter overlap, the in-pulse feature selected as the parameter has become a trend of radar waveform sorting technology in recent years [6]–[12].To get the in-pulse features, some extraction such as Short-Time Fourier transform (STFT) [6], [10] Choi-Williams distribution (CWD) [7] and Wigner-Ville Distribution (WVD) [8] can get the time-frequency feature of radar emitter signals. For the extracted features in two-dimensions or multi-dimensions, some classification algorithm such as Support Vector Machine (SVM) [7], [12] CNN [8], Long Short-term Memory (LSTM) [9] Probabilistic Neural Network (PNN) [10] and Back Propagation Neuron Network (BPNN) [11] have been used to sort the radar waveform and achieved a high accuracy rate. However, for the classifiers in deep learning networks waveform signals, the high classification accuracy has achieved with cost of abundant of training data and training time. Deep learning often requires that each category in the sample database needs to be independent and identically distributed. For the radar waveform received in the actual environment, it is necessary research for us to identify whether it is a known signal or an unknown new signal in a relatively short time. In the field of transfer learning, the main goal is to transfer the learned knowledge to unknown areas. Although learning in the unknown domain is a bit difficult, it can make full use of the knowledge of the known domain and combine the hidden information between the two domains. Transfer learning is involved in image classification, remote sensing image analysis [15], [16], tongue image medical diagnosis and treatment [19], power data mining [20], bearing fault diagnosis [21], [22] and the applications provide research directions for the identification of unknown signals. Literature [14] adopted a scalable model update mechanism based on transfer learning technology to adapt to the increasing number of plant species. After the two transferring operations, The Alexnet which could recognize 15 plants images recognize up to 206 species, and the accuracy rate of that exceed 80% from 60%; Literature [15] uses the form of shared autoencoder parameters for transfer learning, and conducts disjoint training and testing on four data sets of AwA, CUB, aPY and SUN. The knowledge acquired from the three data sets is tested on the other data set. The recognition accuracy rates of the four data sets are 85.09%, 66.25%, 56.69% and 86.94% respectively; Literature [16] which was based on transferring knowledge and saving data structure solved the problem that there is no intersection between known types and unknown types in cross-domain image classification. The average accuracy of the four types image databases is 79.1%. In remote sensing image analysis, literature [17] aiming at the problems of in recognition, ''same object with different spectrum'' and ''foreign object with same spectrum'', transferred the model and parameters of Inception-V3 network and performed high-precision classification and stable process in AID and NWPU-RESISC45. Literature [18] transferred the priori information of ground object classification in historical remote sensing samples to the target model. an improved Bayesian neural network transfer learning was constructed and achieved good results. Literature [19] used the trained image classification network Inception_V3, ResNet18, and ResNet50 to extract the feature value of the tongue image on the preprocessed facial image. The average recognition accuracy rates were 85.30%, 92.84%, and 94.88% respectively. In terms of power data mining, the literature [20] used the maximum mean difference (MMD) to make the source field and the target field as close as possible, deep learning networks such as the Stack Sparse Auto-Encoder (SSAE), LSTM, Gate Recurrent Unit (GRU) were adjusted to obtain data feature mining for fault detection, fault diagnosis and load forecasting. In analysis of diagnosing bearing, literature [21], [22] introduced an auxiliary bearing data set which is similar to the target data set to obtain the target bearing vibration indirectly, the generalization ability of faults were improved under different working conditions; Literature [22] used vibration signals when using vibration signals. The feature data set of bearing detection composed of domain and frequency domain adopts semi-supervised transferring component analysis based on the maximum mean difference embedding method to solve the problem of rolling bearing fault diagnosis under different working conditions.

In the above transfer learning applications, whether network based on freezing and fine-tuning [13]–[19] or transferring component analysis based on the maximum mean difference [20], [22], the learning is transferred from the source domain to the target domain, and the learning and generalization capabilities of the recognition model can be improved. The transferred knowledge from the classification of known waveform signals to the classification of unknown waveform signals provides a direction.

The classification method of radar emitter based on deep learning has strong capacity of resisting disturbance and high identification accuracy [23]–[25]. However, for most of the deep learning, the radar emitter classifiers need to meet the requirements that training data set and the test data set come from the same sample collection and are distributed uniformly [26]. When the source domain and target domain are different or the classification task changes, the transfer learning method is introduced and can transfer the acquired knowledge to other domains [27], [28]. While, in the field of image classification, the bottom deep learning network can generalize common colors and features in natural images [29]. A variety of classical CNN are transferred to different classification tasks, and the training efficiency and classification accuracy of network models are greatly improved [30]–[32]. Various typical CNN such as Alexnet [30], [31] and ResNet [32] have been enough trained maturely to be used in the classification of TFI of radar emitters. In the literature [30], a mixture of pre-trained Encoder (SAE) and AlexNet structures have been used to extract TFI features for the situation where the radar signal sample is small. It can identify 12 radar signals (Costas, LFM, NLFM, BPSK, P1-P4 and T1-T4) with an average recognition rate of 95.5 % when the SNR is greater than −6dB. The GoogleNet network transferred in the literature [31] had realized offline training and online recognition, and could recognize 9 radar signals (CW, LFM, NLFM, BPSK, MPSK, Costas, LFM/BPSK, LFM/FSK, BPSK/FSK). When the SNR was −6dB, the overall average recognition rate could reach 95.5%. These researches are only about the identification of known radar emitters, but there are no relevant researches to solve the identification problem of unknown radar waveform by using the idea of transfer learning.

In this paper, combined with the idea of transfer learning and deep learning network, the obtained neuron units at the full connection layer are used as the reconstruction features of radar emitter signals. One side, the reconstructed feature extractor can convert the initial image into a suitable characteristic of low dimension. The dimensionless neurons unit go randomly through the dropout layer, which can alleviate the fitting degree and are more suitable for the classification of the subsequent tasks. On the other side, by transferring the CNN and keeping the bottom parameters unchanged, we can obtain a group of random neurons to demonstrate special feature difference between known signals and unknown signals.

Among the complex algorithms of deep learning, random forest is an algorithm that integrates the outputs of multiple decision trees for learning after randomly assigning sample size and feature dimensions to all decision trees [33], [34]. For medium high number of dimensions, the random forest can avoid overfitting phenomenon effectively, and its algorithm recognition rate does not change much with the number of feature dimensions [35].

For an image of radar emitter, the original TFI database reflects the distribution of signal energy in time-frequency plane. And for an image-classifier of radar emitter, it reflects signal characteristics through extracting the shape feature of images [32]. The short-time autocorrelation characteristic image database can through the study of the autocorrelation of signal processing of deterministic signal intercept the signal feature, eliminate noise interference [36]–[38], [42]. Fusion of different datasets is a potential solution to improve signal classification accuracy and anti-noise performance. For dual-image database fusion, decision fusion is the highest level of information processing. To determine the appropriate fusion strategy can fuse the advantages of image database and improve the automatic discrimination effect of unknown signals.

The main purpose of this paper is to realize the identification of unknown radar waveform. A sorting identification model based on transfer learning and linear weight decision fusion is proposed. Firstly, the general features of radar signals are extracted by using the known radar samples. Then, based on the transfer learning, the reconstructed features of some unknown signals are taken as the training samples of subsequent classifiers. The difference between known and unknown samples in general feature extraction is used to train the classifier. At the decision level, the weight factor of the dual image database is determined by the overall accuracy of each database to various signals. Finally, the experimental results show that the proposed method is able to identify unknown radar signals under the wide range of SNR. The stability of the recognition model and the high accuracy are verified in several schemes that can simulate the real situation,

Specifically, the contributions of this paper are as follows.

(1) Based on the current status of identifying the known radar emitter signals, the idea of transfer learning is proposed for the identification of unknown emitter signals.

(2) By integrating transfer learning and CNN, a newly reconstructed feature extractor is designed to deeply extract the reconstructed features of known radar emitter signals with higher dimensions and mobility.

(3) Combining the features of the dual image database and utilizing the advantages of the multi-classifier system, the double classifier is fused to make decision output judgment.

II. BASIC FRAMEWORK FOR UNKNOWN RADAR IDENTIFICATION

In this section, this paper gives a basic framework for the identification of unknown radar emitters based on transfer learning and CNN. The configuration of the verification algorithm environment and the preprocessing for selected signal are explained subsequently.

A. TRANSFER LEARNING PROCESS OF UNKNOWN RADAR IDENTIFICATION

In a typical recognition model of radar waveform, the deep learning network can automatically extract data features, but the output sample type labels are limited to known label sets.

When an unknown new type of radar signal appears, the learned knowledge will be acquired and to be transferred to a new classification situation, and it can realize the identification of unknown new class samples [13], [28]. The transfer learning process of unknown new class of radar emitter recognition is shown in Figure 1.

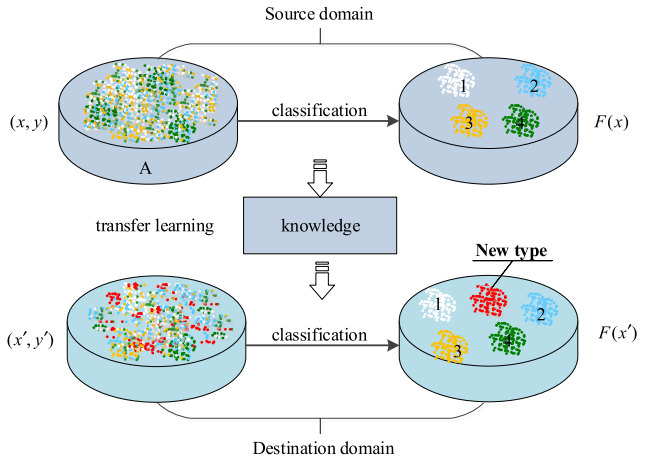

FIGURE 1. The transfer learning process of unknown new class of radar emitter recognition.

As the training process shown in Figure 1, $X = \{x_1, x_2, x_3, \cdots, x_n\}$ is the sample set of the radar waveform, and $Y = \{y_1, y_2, y_3, \cdots, y_p\}$ is the label set to which the signal sample belongs. Suppose $A = \{X, Y\}$ is a training data set of known radar signal. Where, the classification network is trained using the data set A, and the classification function is recorded as $F(\cdot)$, and the output predicted label $F(x)$ is as much as possible true label Y. But in actual testing, when the new type of radar signal (x', y') appears, in other words, $x' \notin X$ and $y' \notin Y$, the model will transfer the existing knowledge to recognize the unknown signal, and predict the signal as its true label y'. The predicted labels set can contain and can be marked a new label.

B. MODEL STRUCTURE OF UNKNOWN RADAR IDENTIFICATION

Different from the literature [30]–[32], the random forest classifier proposed in this algorithm utilizes the neurons output by CNN feature extractor [13], [19]. It can distinguish unknown radar signals automatically after learning the characteristics of unknown signals and known signals. As shown in Figure 2, signals in space are received into the radar signal receiver by the antenna, and the image obtained after signal preprocessing is used as the input of feature extractor. In the feature extraction stage, the CNN is used to extract the general feature of radar signal, and the output neuron group is used as the reconstructed feature vector. In the decision fusion stage, the classifier decision of linear weight fusion of two image data sets is set to recognize the unknown radar waveform.

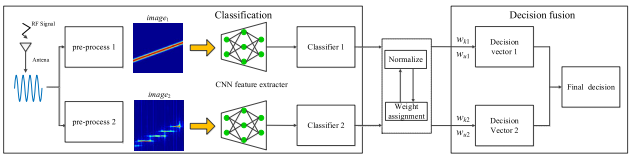

FIGURE 2. Unknown new class of radar emitter recognition transfer learning process.

C. GENERAL SIGNAL PARAMETER SETTING AND PREPROCESSING

1) SIMULATION ENVIRONMENT SETTINGS

When setting the simulation environment, each parameter value of the signal is set as random transformation within the specified range, and the waveform is set as in literature [39]. *mod* (a, b) represents the remainder function, and $\lfloor \cdot \rfloor$ represents the integer downward function. The 11 radar signals defined in Table 1 were simulated in this paper, including LFM, Frank, Costas, P1-P4 and T1-T4. The main work of this paper is that in the case of four known radar signal databases, when a new modulation mode other than the four known modulation mode appears, the system can automatically judge it as a new category. The first four signals in Table 1 (LFM, Costas, BPSK, Frank) are marked as known modulation signals, while other signals are marked as unknown signals. When the signal is simulated, the simulation range is from −6dB to 9dB, and the step is 3dB.

TABLE 1. Radar waveform modulation parameters.

Radar Wave forms	$f[k]$	$\phi_{i,j}$ for sub code
LFM	$f_0 + \frac{B}{\tau p \omega}(kT_s)$	constant
Costas	f_j	constant
BPSK	constant	0or π
Frank	constant	$\frac{2\pi}{\mathrm{M}}(2i-1)(j-1)$
P1	constant	$-\frac{\pi}{\mathrm{M}}[M-(2j-1)][(j-1)M+(i-1)]$
P2	constant	$-\frac{\pi}{2\mathrm{M}}[2i-1-M][2j-1-M]$
P3	constant	$\frac{\pi}{\rho}(i-1)^2$
P4	constant	$\frac{\pi}{\rho}(i-1)^2-\pi(i-1)$
T1	constant	$\mathrm{mod}\left(\frac{2\pi}{\mathrm{N}_{ps}}\left\lfloor N_g(kT_s - j\tau_{pw})\frac{j\mathrm{N}_{ps}}{\tau_{pw}}\right\rfloor, 2\pi\right)$
T2	constant	$\mathrm{mod}\left(\frac{2\pi}{\mathrm{N}_{ps}}\left\lfloor N_g(kT_s - j\tau_{pw})\left(\frac{2j-\mathrm{N}_g+1}{\tau_{pw}}\right)\frac{\mathrm{N}_{ps}}{2}\right\rfloor, 2\pi\right)$
T3	constant	$\mathrm{mod}\left(\frac{2\pi}{\mathrm{N}_{ps}}\left\lfloor \frac{\mathrm{N}_{ps}\mathrm{B}\,(kT_s)^2}{2\tau_{pw}}\right\rfloor, 2\pi\right)$
T4	constant	$\mathrm{mod}\left(\frac{2\pi}{\mathrm{N}_{ps}}\left\lfloor \frac{\mathrm{N}_{ps}\mathrm{B}\,(kT_s)^2}{2\tau_{pw}} - \frac{\mathrm{N}_{ps}\mathrm{B}kT_s}{2}\right\rfloor, 2\pi\right)$

For the design of feature extractor, the four kinds of signals generate 2,500 samples at each SNR, and then the 2,500 samples generated are distributed to the training set and the test set respectively in a 4:1 ratio. Therefore, there are 48,000 samples in the feature extractor's training set and 12,000 samples in the test set; For the design of the classifier, the four known signals generate 1000 samples at each SNR, and then are distributed to the training set and the test set respectively in a ratio of 1:1. The unknown eight kinds of signals generate 500 samples under each SNR, and then the 24,000 samples are distributed to the training set and the test set respectively according to the ratio of 1:1 with different signal types. Therefore, there are 24,000 samples in the training set and 24,000 samples in the test set.

2) CWD TIME-FREQUENCY ANALYSIS TECHNOLOGY

The radar emitter signal is a typical non-stationary signal. The time-frequency analysis (TFA) technology can describe the change of the frequency spectrum content of the signal in the time domain. And it can extract the effective information to the maximum extent by mapping the one-dimensional time domain signal to the two-dimensional time-frequency surface. Among the many TFA processes, WVD is the most basic analysis technology with a high time-frequency resolution [40]. However, in the processing of multi-component signals, there are serious cross-term influence and low anti-noise performance. The TFA of Cohen class can be obtained by smoothing WVD with different kernel functions $\psi(t,\tau)$. And the analysis can compromise the cross-restriction of cross-terms and obtain high time-frequency resolution. For a given time-frequency signal, the Cohen distribution of it is defined as follows:

$$C_y(t,f) = \iint y\left(u+\frac{\tau}{2}\right) y^*\left(u-\frac{\tau}{2}\right) \psi(t-u,\tau)\, e^{-j2\pi f\tau}\, du\, d\tau \quad (1)$$

Given different kernel function calculation expressions, different functions will be obtained. Based on the nonlinear time-frequency CWD distribution [41], its kernel function is expressed as follows:

$$\psi(t,\tau) = \frac{1}{\sqrt{4\pi\alpha\tau^2}} \exp\left(\frac{1}{4\pi\alpha\tau^2} t^2\right) \quad (2)$$

where, α is the scaling factor. It is a zero-dimensional parameter to measure the influence of cross-suppression and time-frequency resolution.

The time-frequency distribution CWD will be obtained when formula (2) is bought into the Cohen formula, and is expressed as CWD $(\cdot)$. For a given signal $y(t)$, its CWD distribution is expressed as follows:

$$CWD_y(t,f) = \iint y\left(u+\frac{\tau}{2}\right) y^*\left(u-\frac{\tau}{2}\right) \frac{1}{\sqrt{4\pi\alpha\tau^2}} e^{\frac{1}{4\pi\alpha\tau^2}(t-u)^2 - j2\pi f\tau}\, du\, d\tau \quad (3)$$

This article sets $\alpha = 1$ to balance the relationship between CWD cross-term suppression and time-frequency resolution.

3) TIME-FREQUENCY IMAGE DATABASE

Now We analyze a simplest radar transmitting and receiving system. The radar emitter signal reaches the receiver through a channel. The received signal $y(k)$ of the receiver can be expressed as follow:

$$y(k) = s(k) + w(k) \quad (4)$$

where, $s(k)$ represents the ideal discrete signal after intermediate frequency sampling, and n (k) represents additional Gaussian white noise (AGWN), k is an index value that increases sequentially with the sampling interval.

The transmitted signal $s(k)$ can be expressed as the following:

$$s(k) = Ae^{j\theta(k)} = Ae^{j(2\pi f(k)(kT_s)+\phi(k))} \quad (5)$$

where, A represents the instantaneous envelope (amplitude) of the ideal sampled signal, $\theta(k)$ represents the instantaneous phase of the ideal sampled signal, $f(k)$ is the instantaneous frequency, k is the sampling index value, T_s is the signal sampling interval, and $\phi(k)$ is the instantaneous phase offset.

CWD is operated to the pulse modulation signal $y(k)$, and based on the performance considerations of the CPU and GPU of the experimental platform, the appropriate signal sampling interval T_s and the number of sampling points k are set to obtain two-dimensional matrix M_Y in size of 64*64. $M_Y(i,j)$ is used to represent the value of the $i-th$ row and the $j-th$ column in that matrix. In order to convert to image, the value of each pixel in the image is calculated and expressed using the normalization method

$$TFI(i,j) = 255\frac{M_Y(i,j) - \min(M_Y)}{\max(M_Y) - \min(M_Y)} \quad (6)$$

where, max $(\cdot)$ and min $(\cdot)$ represent the maximum and minimum values of the two-dimensional matrix. So far, an original TFI of the size of the signal modulation characteristic is obtained. The original TFIs (SNR = 0dB) are shown in Figure 3.

4) SHORT-TIME AUTOCORRELATION FEATURE IMAGE DATABASE

Directly performing CWD time-frequency analysis to the received unstable pulse-modulated signal $y(t)$ can obtain the original TFI, but the original TFI characterizes the feature of the noise signal, too. Now, seeks a feature representation that can highlight the received useful signal [36] and signal recovery [37].

Observation shows that the radar signal can be regarded as stable in a short time and can be approximately unchanged. Using its short-time stationarity, the stable signals of each segment are approximated by extracting a finite length part of the radar signal using a window function. There are two commonly used window functions, one is a rectangular window, the function is as follows:

$$w(n) = \begin{cases} 1, & 0 \le n \le N-1 \\ 0, & \text{else} \end{cases} \quad (7)$$

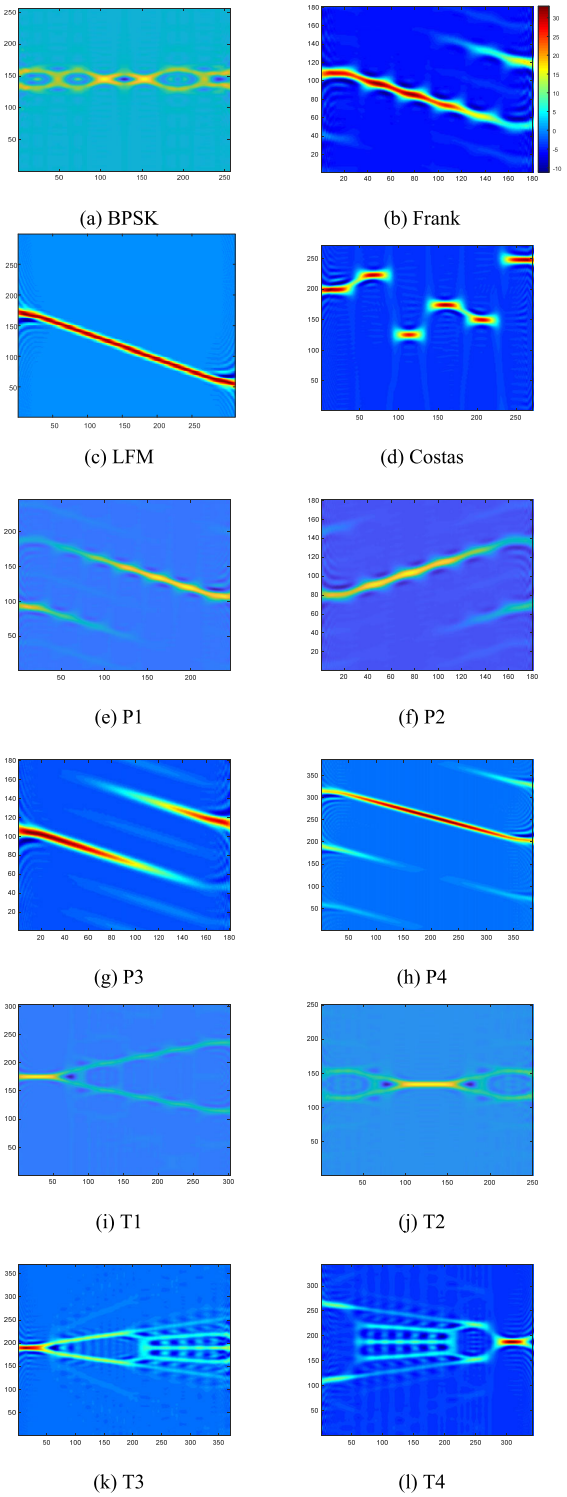

FIGURE 3. Original time-frequency images of the 12 signals in Table 1 (SNR = 0dB).

The other is the Hamming window, whose function is as follows,

$$w(n,\alpha) = (1-\alpha) - \alpha cos\left(\frac{2\pi n}{N-1}\right),\ 0 \le n \le N-1 \qquad (8)$$

In general, α is taken as 0.46.

Windowing is mainly to reduce leakage, and a window function with narrow main lobe width and large side lobe attenuation should be selected. This approach also has some limitation. Since the single window is applicable to all frequencies, the resolution of the analysis is the same for all points in the time-frequency field. Therefore, it is almost impossible to obtain any high resolution in time and frequency. By comparison, the width of the main lobe of the rectangular window is smaller than that of the Hamming window, and it has a higher spectral resolution, but the side lobe peak of the rectangular window is larger, so its spectral leakage is more serious. The width of the main lobe of the Hamming window is wider, about twice that of the rectangular window, but its side lobe attenuation is larger, with a smoother low-pass characteristic, which can reflect the frequency characteristics of short-time signals to a higher degree. Determine an appropriate window function to get a frame of length of M, and the internal signal of the frame structure remains stable. It should be emphasized that although the continuous segmentation method can be used for framing, the overlapping segmentation method (shown in Figure 4) must be used, because such a framing method can ensure a smooth transition from frame to frame and maintain its continuity to ensure that data is not lost. Usually the overlapping part of the previous frame and the next frame is called frame shift. The ratio of frame shift and frame length is generally taken as $0 \sim 1/2$. The schematic diagram of frame shift and frame length is shown in Figure 4.

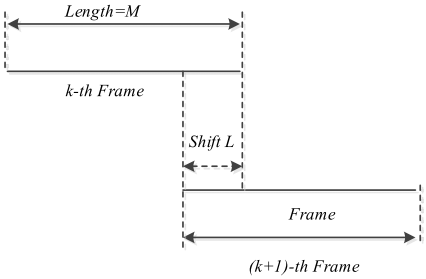

FIGURE 4. Acquisition of signal framing.

After obtaining a stable framed signal, since the values of the deterministic signal at different times generally have a strong correlation. For the interference noise which is with strong randomness, the correlation of the values is generally weak at different times. So, the difference can be used to distinguish the deterministic signal in the sub-frame from the interference noise.

The autocorrelation processing is operated on the signal side $y(t)$, and the autocorrelation $R_y(\tau)$ is:

$$\begin{aligned} R_y(\tau) &= E[y(t)\,y(t-\tau)] \\ &= E\{[x(t)+w(t)]\,[x(t-\tau)+w(t-\tau)]\} \\ &= E[x(t)\,x(t-\tau)] + E[w(t)\,w(t-\tau)] \\ &\quad + E[x(t)\,w(t-\tau)] + E[w(t)\,x(t-\tau)] \\ &= R_x(\tau) + R_w(\tau) + R_{xw}(\tau) + R_{wx}(\tau)\,R_y(\tau) \\ &= R_x(\tau) + R_w(\tau) \end{aligned} \qquad (9)$$

Since the noise $w(t)$ is not related to the signal $x(t)$, then, there is

$$R_y(\tau) = R_x(\tau) + R_w(\tau) \tag{10}$$

For the zero-mean Gaussian white noise $w(t)$ with a wide bandwidth, the autocorrelation $R_w(\tau)$ is mainly reflected in the vicinity $\tau = 0$. When τ is larger, it mainly reflects the situation of $R_x(\tau)$, so there is:

$$R_y(t) \approx R_x(t) \tag{11}$$

It can also be explained above that for the received signal $y(t)$ superimposed with noise, when the time delay τ of its autocorrelation function $R_y(\tau)$ is large, the contribution of random noise to $R_y(\tau)$ is small, and then $R_y(\tau)$ mainly express the characteristics of the deterministic signals contained in $y(t)$. For non-periodic random noise, when the time delay τ is large, the autocorrelation function of the noise term tends to zero, which can extract useful signals from the noise [42]. In general, it is more complex to restore a noise-contaminated signal than detecting the presence of known signals in the noise. And if the noise-covered signal appears only once, rather than appears repeatedly, the methods such as sampling-integrals and digital-averaging cannot be used to restore the signal. This autocorrelation processing is not to recover the signal polluted by noise, but to extract the features of the useful signal directly, which is very useful in this case.

According to the analysis to signal above, the method the short-time autocorrelation feature image (SAFI) is adopted to transform the received signals. The construction of feature images is constituted by the following steps, and the diagram of the construction above in Figure 5.

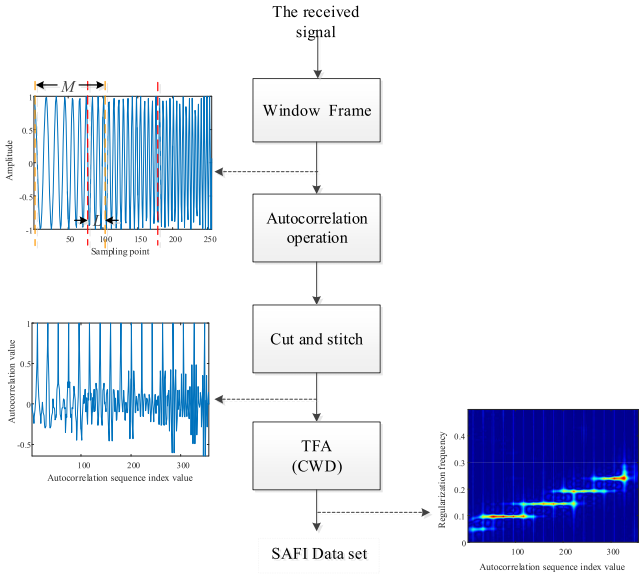

FIGURE 5. Construction process of short-time autocorrelation feature image.

The specific details are explained below. In the stage of frame acquisition, for the mixed sampled signal $y(k)$ with length of N, the signal is divided into several frames by a rectangular window of length of M, then the length of each frame signal obtained is M. If the last frame is not full, the insufficient part will be added with zero padding operation; in the frame signal auto-correlation sequence generation stage, for each frame signal with length of M, auto-correlation length of that is $2M - 1$, the final auto-correlation sequence is obtained by intercepting its fragments in range of $(M/2, 3M/2)$; in the frame stitching stage, due to the difference in autocorrelation values of each subframe, after normalizing each subframe, splicing frame by frame to obtain the autocorrelation sequence of the sampled signal; in the generation stage of autocorrelation feature image, the obtained short-term autocorrelation features are processed by the CWD time-frequency transformation introduced in section II-C-2. After that a characteristic image that can specifically feature of signals has been obtained. In the image pixel size, choose the same size as the original time-frequency image. As the Hamming window has a smoother low-pass characteristic, which can better reflect the characteristics of short-term signals. After the Hamming window is selected, and feature images obtained have a better pixel distribution. The 12 signals in Table 1 are processed as above, and SAFIs of those are shown in Figure 6.

It should be further explained that the SAFI of radar signal used in this section is obtained by autocorrelation sequence with CWD time-frequency analysis. some related knowledge the signal autocorrelation value such as the deviation analysis the sample point parameters and the clipping rules are all introduced in 3.1.4 of the literature [36] completely and in detail.

III. REALIZATION OF THE UNKNOWN RADAR WAVEFORM IDENTIFICATION FUNCTION

To achieve the identification of unknown new types of radar emitter, a recognition algorithm using decision fusion after transfer learning reconstruction feature extraction is proposed in this paper. The network is divided into two parts, reconstruction feature extraction and decision fusion.

A. RADAR SIGNAL FEATURE EXTRACTION

An accurate feature extraction is the basis to ensure the validity and rationality of the classification algorithm. Increasing the feature dimension by an appropriate amount can obtain the better signal parameter characteristics. In the field of image recognition, CNN uses the generalization of common colors and features in natural images to achieve perfect results [29]. The image set of two-dimensional TFI achieve feature extraction by using CNN. The idea is based on the concept of deep transfer learning, the reconstruction and extraction of feature are realized by transferring some parameters [13]. The Original TFI or the SAFI which is obtained by preprocessing the received signal is used as the input of CNN. The diagram of reconstruction feature extraction is shown in Figure 7.

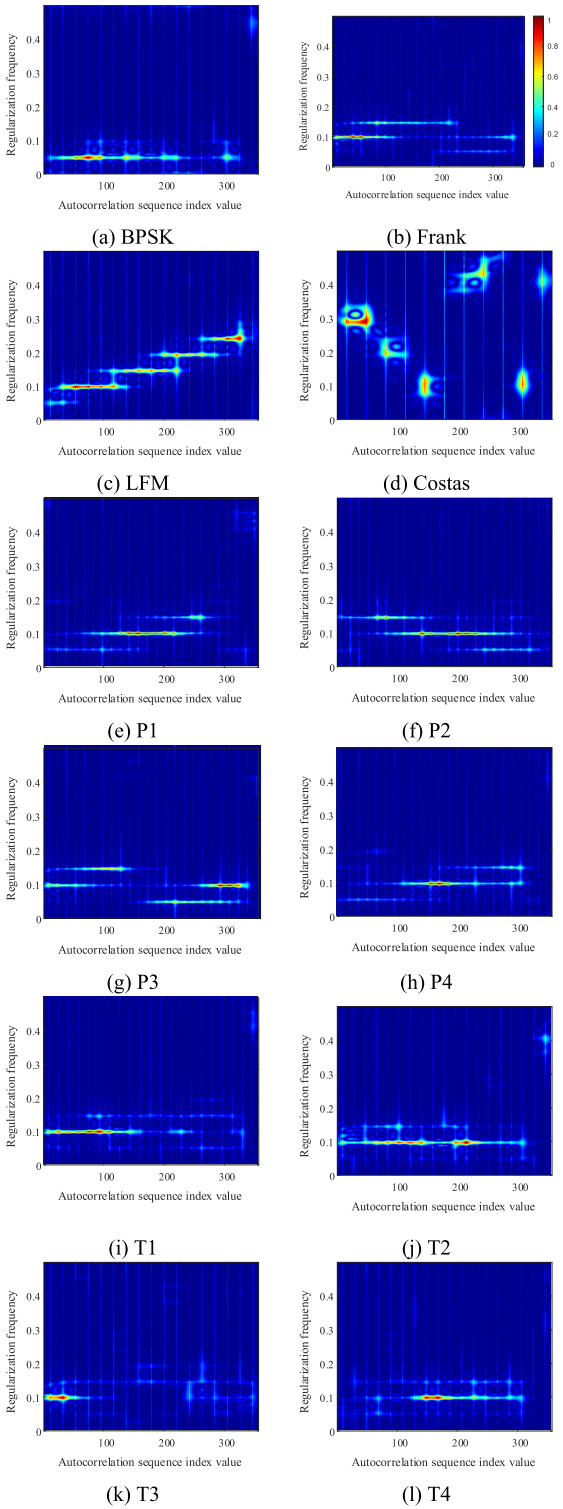

FIGURE 6. The short-time autocorrelation feature image of 12 signals (SNR = 0dB).

The reconstructed-feature extraction based on transfer learning is to realize the accurate classification of known radar emitters and the accurate extraction of reconstructed features. As shown in Figure 7, the classification of unknown radar signal waveform in the whole process consists of three steps.

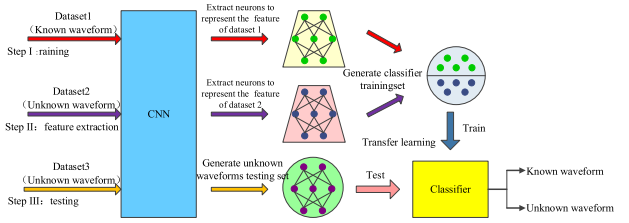

FIGURE 7. Transfer learning reconstruction feature extractor.

The first step is called the training stage. The data set 1 (LFM, Costas, BPSK and Frank in Table 1) conducts parameter training for CNN classified network. After training a large-scale data set, the parameters in CNN fit the data set 1 (known radar signal characteristic image) extremely. Based on obtained training results, the neurons in the full connection layer of CNN (that is, 256 neurons in the Figure 8) can show the characteristics of each sample of the known radar signal datasets 1.

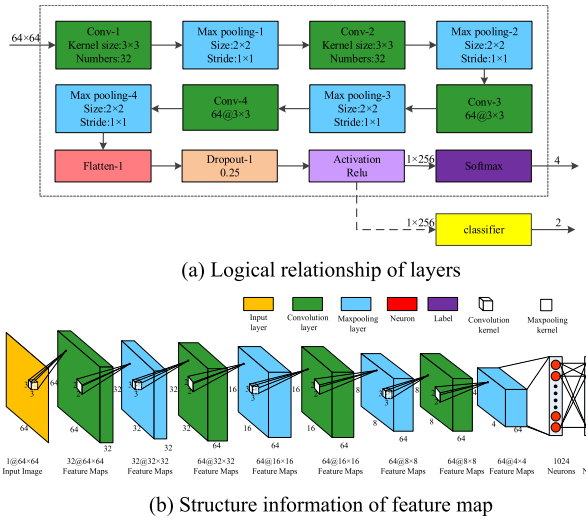

(a) Logical relationship of layers

(b) Structure information of feature map

FIGURE 8. CNN architecture of radar emitter feature extraction.

The second step is the feature extraction stage. The data set 2 (P3, P4, T3 and T4 signals in Table 1) is used as the test input of the trained CNN network. The 256 neurons extracted from the full connection layer of CNN represent the feature of each sample in data set 2. It should be noted that the signal type of data set 2 is completely different from that of data set 1. Since data set 2 does not participate in the training of CNN, it is "unknown" to the trained CNN. After step 1 and Step 2, we obtain the characteristic representation of known signals and unknown signals from CNN, and complete the classifier training with the training set marked as known signal and unknown signal. So far, we can determine whether the test signal is a known signal or an unknown signal.

The third step is the testing stage. The data set 3 (signals P1, P2, T1 and T2 in Table 1) tests the recognition effect of unknown signals of the transfer learning network model. It should be noted that the signal type of data set 3 is different from that of data set 1 and data set 2. Data set 3 does not

participate in CNN training and is ''unknown'' to CNN. During the test stage, 256 neurons in the full connection layer of CNN are extracted as the feature representation of each sample in data set 3, and then the feature representation was input into the classifier trained in Step 2 to verify the model's ability to automatically distinguish unknown signals from the results of the classifier. In order to avoid model overfitting, signals of data set 1, during testing and training. data set 2 and data set 3 are extracted in random order respectively.

CNN and Softmax classifier are trained with the four known radar signals in dataset 1. The network structure and the size of the characteristic layers obtained by each layer are shown in Figure 9.

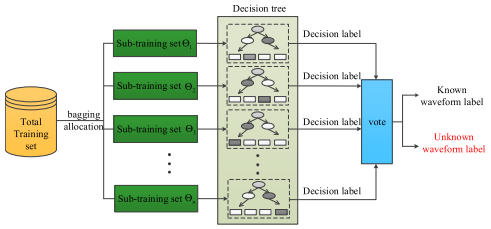

FIGURE 9. Structure of random forest algorithm.

As shown in Figure 8.a, the input TFI is input to four convolutional layers, four pooling layers and the fully connected layer. The output 256 neurons (in Figure 8.b) which are activated by Relu function are the reconstructed features. The structure of CNN is relatively simple. It mainly composed of the convolutional layer, the maximum pooling layer, the fully connected layer, and the dropout layer. Among them, the dropout layer will discard neurons from the former layer randomly. The value of the drop probability is set as 0.25 to prevent network overfitting [43]. As the relevant parameters of the training time and accuracy of the neural network are the learning rate, the size of the convolution kernel, the number of iterations, and the batch of training samples (abbreviated as batch size). By the method that changing a single variable at one time, a structure with high accuracy and appropriate time consumption can be obtained. The training signal samples are chosen from the SNR of −6dB to 9dB, and the test set uses the signal with a SNR of 0dB for testing. Under the simulation condition of GTX1050TI GPU, after 10000 iterations, the final hyperparameter configuration of the network model is obtained as below: block size is 128, convolution kernel size is 3×3, learning rate is 0.0001.

B. DUAL IMAGE DATABASE DECISION FUSION

Based on the dual image databases in 2.3, the image fusion theory is considered to extract features from TFI and SAFI respectively. And the outputs of the two classifiers are fused in parallel mode as the final classification decision. Decision fusion is the process of information fusion from multiple data sources after preliminary classification of each data source [44]. As an important part of unknown signal recognition in this paper, fusion strategy is mainly determined by the output form of classifier and the cost of sample training [45]. Nowadays, the research on decision fusion model focuses on a variety of combinations of classifier systems. According to the constructed database, classification decision and information fusion are performed at different information levels to overcome the limitation of low accuracy of single classifier [46]. For the decision fusion of double classifier, a linear weight allocation technique based on recognition accuracy is adopted in this paper. Firstly, based on the recognition performance of unknown signals and known signals in each data set, the weight factor of the classifier is determined. And then the classification probability value output by the classifier is combined with the weight factor linearly.

Generally speaking, the output levels of classifiers can be divided into three levels: abstract level, rank level and measurement level. The abstract layer refers to the number of the predicted category of the sample output by the classifier. the rank level refers to the number sequence of the predicted category of the sample output according to the possibility of the category. The measurement layer refers to the possibility of all categories of the sample output by the classifier [47]. In terms of the amount of information, there is a reduction process of an information from the measurement layer to the abstract layer. In addition, the decision fusion effect based on the measurement level performances better. Assuming that classification classifier have n classes, the initial probability of the signal in TFI database $T_i = \{T_1, T_2, T_3, \ldots, T_n, i = 1, \ldots, n\}$ shows the probability of each category, and the initial classification result of the signal in the SAFI database is $S_i = \{S_1, S_2, S_3, \ldots, S_n, i = 1, \ldots, n\}$. The weights of two databases the above for each class after normalization are $W_{T_i} = \{W_{T_1}, W_{T_2}, W_{T_3}, \ldots, W_{T_n}, i = 1, \ldots, n\}$ and $W_{S_i} = \{W_{S_1}, W_{S_2}, W_{S_3}, \ldots, W_{S_n}, i = 1, \ldots, n\}$ respectively. Then the classification result after decision fusion is calculated as below:

$$P_i = T_i \times W_{T_i} + S_i \times W_{S_i} \tag{12}$$

where, P_i are the probability of the i-th class after fusion, T_i represents the probability of the i-th class of TFI database, S_i represents the probability of the i-th class of the SAFI database, W_{T_i} represents the linear weight of the i-th class of the TFI database, W_{S_i} represents the linear weight of the i-th class of the SAFI database.

The types of radar emitter in this article are divided into known radar waveforms and unknown radar waveforms (i.e. $n = 2$). the weight value and weight of each database are determined by the accuracy of the recognition of the known radar waveform and the unknown radar waveform when each classifier is used alone. that the recognition accuracy rate ranges from 0% to 100%. The range of values is [0, 1].So for the data of TFI(can be regarded as classifier 1), the recognition accuracies of the known radar waveform and the unknown radar waveform are P_{T_1} and P_{T_2}.And for the data of SAFI(can be regarded as classifier 2), the recognition accuracies of the known radar waveform and the unknown

radar waveform are P_{T_1} and P_{T_2} he classifier using the short-time autocorrelation feature image (defined as classifier 2), so we can obtain the weights for the TFI database by the following formulas.

$$W_{T_1} = \frac{P_{T_1}}{P_{T_1} + P_{S_1}} \tag{13}$$

$$W_{T_2} = \frac{P_{T_2}}{P_{T_2} + P_{S_2}} \tag{14}$$

where, W_{T_1} is the normalized recognition accuracy of TFI database for known radar waveform, i.e. the weight value, W_{T_2} is the normalized recognition accuracy of TFI database for unknown radar waveform. By the similar method, the weight value of SAFI database to the known signal W_{S_1} and unknown signal W_{S_2} can be obtained. The calculations are given as below.

$$W_{S_1} = \frac{P_{S_1}}{P_{T_1} + P_{S_1}} \tag{15}$$

$$W_{S_2} = \frac{P_{S_2}}{P_{T_2} + P_{S_2}} \tag{16}$$

C. RANDOM FOREST ALGORITHM

According to the dimensions and features of the reconstructed features obtained in the section III-A, the selected base classifier is introduced in this section.

Random forest [48] is a learning method based on Bagging integrated learning theory and random subspace method. The random forest which is consisting of several decision trees can aggregate the advantages of decision trees and solve the problem of restricting the processing of complex data. In addition, it has good parallelism and expansibility in high-dimensional data classification and tolerances for noise and outliers. With the high learning efficiency, it is often used in high-dimensional big data classification. Based on the thinking of unweighted selection proposed by Leo Breiman, the training samples for the decision trees are select randomly by the bagging mechanism. As the selection are operated with the return, there will be a possibility of overlapping between the sub-training sets. The feature variables are also chosen randomly to avoid the problem of sample coincidence. Thus, the samples and decision trees modeled by the samples are both different from each other.

The training set for random forest is consisting of the radar signals features obtained by CNN. The structure of the random algorithm is shown in Figure 9, which is mainly composed of three parts, the sub-training set of each decision tree, the nodes of each decision tree and the random forest formed by summarizing the results.

As shown in Figure 9, the total training set are set as $A = (X, Y)$, where, X represents the signal sample set and Y represents the signal label set. For a random forest with t decision trees, each decision tree is modeled as follows: first, conduct bagging resampling to form the sub-training set Θ_i for the i-th decision tree; Then random feature tailoring is carried out for each signal sample in the sub-training set, and feature number is m. Thus, the construction of nodes in each decision tree is completed.

When the test sample S is input, the result of i-th decision tree is decided by the sub-training set Θ_i generated randomly by the according to the total training set A and is expressed as The random forest summarizes the results of the decision tree classifier $\{h(S, \Theta_i), i = 1, 2, 3, \cdots, t\}$ and uses majority voting method to output the final classification results. The prediction result of the random forest depends on the decision categories of all decision trees. The decision tree conducts a majority vote and $h(S, \Theta_i)$ outputs the most categories as the categories to which the test set samples belong [49]. For the test samples S, the probability of it is classified to label Y is expressed as $P_{RF}(S, Y)$ and is calculated as below:

$$P_{RF}(S, Y) = \frac{1}{t} \sum_{i=1}^{t} I(h(S, \Theta_i) = Y) \tag{17}$$

where, $I(\cdot)$ is the indicator function, if $\cdot$ true, it takes the value 1, otherwise it takes the value 0; t is the number of decision trees in the random forest; $h(S, \Theta_i)$ is the decision result of the decision tree. According to the output classification probability vector, the highest probability is selected as the classification category of the test signal sample. Then the classification function $G_{RF}(S)$ of the random forest for the test sample S can be expressed as

$$G_{RF}(S) = \arg\max_{Y}(P_{RF}(S, Y)) \tag{18}$$

where, $P_{RF}(S, Y)$ is the probability of sample to category, and $\arg\max_{Y}(\cdot)$ is the parameter of output maximum value.

For a certain training set, the number of decision trees t and the number of features m both affect the accuracy and loss value of the random forest model. As a base classifier for random forests, the greater the difference between decision trees, the better the results we will get. and the difference between decision trees can be enhanced by adjusting the number of t. With the classification accuracy of the algorithm as the target, the number of decision trees is determined $t = 101$ based on the various loss functions. It should be noted that when training the nodes of each decision tree, the features used are extracted from all features (total number is M) randomly according to a certain proportion without replacement. For the setting of the number of feature subsets m, according to Leo Breiman's suggestion, can be set as the three gradients: $1/2\sqrt{M}, \sqrt{M}, 2\sqrt{M}$. In this paper, the signal samples after feature extraction are represented by 256 neurons, i.e. M=256. The random forest classifier effect is tested, according to the conditions of 8, 16, and 32. The TFI dataset is used to set the parameter of random forest model. The simulation range is from −6dB to 9dB at an interval of 3dB. 4 types of known waveforms are composed of LFM, Costas, Frank, BPSK, T1, T2, P1, P2 are marked as unknown waveforms for training. And T3, T4, P3, P4 are marked as unknown waveforms for testing. The other simulation conditions are stated in section II-C-1. The recognition accuracy results are shown in Table 2.

TABLE 2. The selection of the feature number.

No	Tree number	Feature number	Accuracy
1	101	8	67.88%
2	101	16	67.39%
3	101	32	66.25%
4	101	256	66.68%

Analysis of the data in Table 2 shows that when the number of decision trees remains the same, the number of features is changed according to the three gradients. When the number of sub-features is 8, the model recognition accuracy reaches the highest. Considering the calculation amount and accuracy, the number of decision trees is set to be 101 and 8 sub-features are chosen to model the decision tree. So far, for the identification of unknown signals, the best state of the model is selected.

IV. EXPERIMENTAL RESULTS AND ANALYSIS

A. DOUBLE DATABASE LINEAR WEIGHT DETERMINATION

The implementation stages of the entire classification model described in section III-A includes the training stage, the unknown feature extraction stage and test the transfer learning network.

The dataset 1 (the original TFI of the four signals of LFM, Costas, BPSK, and Frank) is used to train the CNN, then the classification result and the neurons of known signal can be obtained from the CNN. The data set 2 (the original TFI of the four signals P3, P4, T3 and T4) are input to the CNN to get the 256 neurons of the fully connected layer in the CNN. At the CNN level, the four signals in dataset 2 are unknown signals compared to dataset 1. The two above groups of neurons obtained are used to train the classifier. Then, the data set 3 (the original TFI of the four signals P1, P2, T1 and T2) are also input to the CNN to get the 256 neurons of the fully connected layer in the CNN. The obtained 256 neurons are then input into the trained hybrid classifier to determine whether the target signal is known or unknown. After the above three stages, the obtained classifier is labeled as Scheme 1. For comparison, Then, the original TFI data set is changed to the STFI data set data set. After the similar three stages, the obtained classifier is marked as scheme 2. According to the simulation conditions introduced in section II-C-1, the test set is consisting of eight signals. And each signal has 500 samples at each SNR. When the SNR is 0 dB, the test results of the eight signals at 0 SNR are shown in Figure 10.

After observation of Figure 10, it can be found that under the two schemes these eight test signals have different recognition effects. For the first four types of signals, the accuracy rates between the two schemes have little difference, and the accuracy rate of the recognized signals is close to 100%; For the latter four types of signals, the performance between the two schemes is different, scheme 1 performances better in recognizing the T1 and P1 signal, while scheme 2 performances better in recognizing the T2 and P2 signal. On the whole, accuracy rate of unknown signal is in the interval

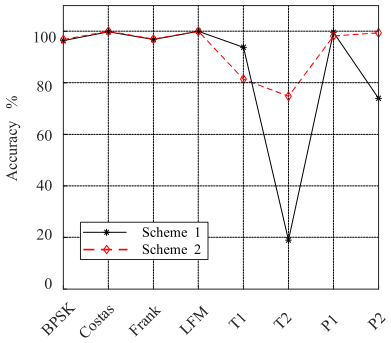

FIGURE 10. The recognition accuracy of eight test signals by the two schemes (SNR = 0 dB).

[70%, 100%]. The advantages of Scheme 1 and Scheme 2 are not average in different signals. And it is not wise to use only single scheme to identify unknown signals. The performance of the known and unknown signals by the two databases are aggregated and shown in Table 3.

TABLE 3. The recognition rate of two databases for unknown and known signals.

Name of dataset	The types of the signals	
	Known radar waveform (LFM、BPSK、Frank、Costas)	Unknown radar waveform (T1、T2、P1、P2)
TFI	98.30%	71.63%
SAFI	98.46%	88.42%

After analyzing the data in Table 3, we find that the two types of image databases have different classification effects for known and unknown signals. Based on formulas (13)-(16), the linear weights of the two classifiers for known and unknown signals are calculated and shown in Table 4.

TABLE 4. The linear weight of two databases for unknown and known signals.

Name of dataset	Known radar waveform	Unknown radar waveform
TFI	0.50	0.45
SAFI	0.50	0.55

When the classifiers trained by the two image databases produce different decisions, as shown in Figure 11, the model can give a final decision.

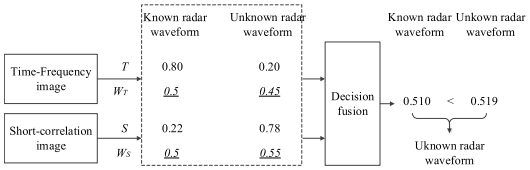

FIGURE 11. The decision fusion diagram.

B. RECOGNITION ACCURACY OF FUSION MODEL

The original TFI database and the SAFI database are fused to complete the training, feature extraction and testing stages

to achieve identifying the unknown radar waveforms. The decision fusion model is introduced in III-B and the linear weight values of the two databases are given in IV-A The test results of the classification model are shown in Table 5.

TABLE 5. The results of decision fusion classification model.

The types of the signals	-6dB	-3dB	0dB	3dB	6dB	9dB
Known radar waveforms (LFM、BPSK、Frank、Costas)	99.45%	99.31%	99.22%	99.15%	99.35%	99.35%
Unknown radar waveforms (P1、P2、T1、T2)	80.31%	80.75%	80.83%	81.32%	80.65%	80.55%

It can be found from the data in Table 5 that the recognition rate of the decision fusion classification model for the known radar waveform is higher than that of the unknown radar waveform. The accuracy of the known radar waveform can reach more than 99.15%, and the accuracy of the unknown radar waveform is in the interval (80%, 81%), which shows that the known signal and the unknown signal can be better distinguished. After observing the change of accuracy under different SNRs, the accuracy of unknown signals and known signals performance almost the same characteristics at different SNRs, which can indicate that the neurons extracted in the CNN-trained data set are not trained by CNN. It can be explained that there is a difference between the neurons the trained CNN and the neurons extracted from non-trained CNN. And it is feasible to use this difference to distinguish the known and unknown radar waveforms.

To illustrate specifically the superior performance of the decision fusion model, a Neuron Mix model is introduced for comparison. After the feature extraction stage, the neural output of the dual database of the original TFI database and the SAFI database is mixed. Under the simulation conditions of IV-A, the recognition results of the TFI database, neuron mix model and decision fusion model are shown in Figure 12.

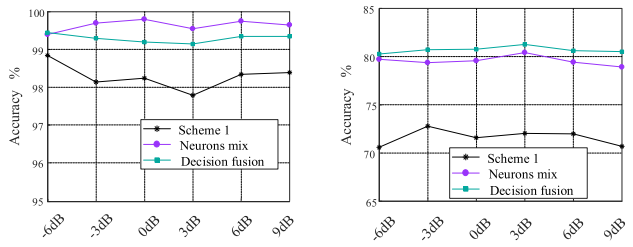

(a) Known signal accuracy (b) Unknown signal accuracy

FIGURE 12. Comparison of results of multiple classification models.

As shown in Figure 12, in the recognition of known signals (a), the neuron mix model has the highest accuracy, followed by the decision fusion mode. And for the recognition of unknown signals (b), the decision fusion model has the highest accuracy, followed by of Neurons Mixed model. The recognition accuracy of the three classification models showed consistency under different SNRs, which can further indicate that the classification results are acceptable. We can see that no matter for recognizing the known signal or an unknown signal, the decision fusion model and the neuron mix model are better than the original TFI database (Scheme 1). For the recognition of known signals (a), the neuron mix model is always better than decision fusion, but in the recognition of unknown signals (b), the neuron mix model is not as obvious as decision fusion. In the context of the actual application of waveforms, to capture the unknown radar., choosing a decision fusion model can effectively distinguish between known and unknown radar waveforms.

C. ANTI-ALIASING PERFORMANCE ANALYSIS OF FUSION MODEL

In section IV-A, when the original TFA database is used by alone, the obtained recognition result of the T2 signal is not optimistic (see Figure 10 for details). To analyze and solve this case, the confusion matrix of all signals is studied further. For the original TFI database, the confusion matrix of testing signals is analyzed o at 0dB (see Table 6).

TABLE 6. Confusion matrix of the original TFI database (SNR = 0dB).

	BPSK	LFM	Costas	Frank	P1	P2	T1	T2
Known	0.96	1	1	0.97	0	0.26	0.06	0.81
New type	0.04	0	0	0.03	1	0.74	0.94	0.19

In Table 6, 8 kinds of signals are to be simulated, they are recognized to be two labels, known signals and unknown signals. At SNR of 0 dB, most of the unknown signals can be identified accurately, in which almost 81 percent of T2 signal is misjudged as the known radar waveform. After observing the CNN parameters of the feature extraction network, it is found that for CNN that have only been trained with LFM, Costas, BPSK, and Frank. When the T2 signal is input, it will 100 percent be judged by the classifier as a BPSK. That is to say, for the non-trained T2 signal, the feature of that is close to BPSK signal. That is why T2 signal is recognized as an unknown signal with low accuracy.

In the analysis of II-C-4, it can be seen that through the construction of the SAFI, a new feature image that can characterize the image uniquely. And from the perspective of signal recognition, the feature of signal is strengthened SAFI. The fusion matrix of the decision fusion of these two image databases at 0 dB is shown in Table 7.

TABLE 7. Confusion matrix for decision fusion (SNR = 0dB).

	BPSK	LFM	Costas	Frank	P1	P2	T1	T2
Known	0.98	1	1	0.99	0	0.01	0.07	0.68
New type	0.02	0	0	0.01	1	0.99	0.93	0.32

From the confusion matrix of the decision fusion classification model, we can find that for the known radar waveforms, the decision the BPSK and Frank signals have

been slightly improved by fusion classification model. And the recognition rate of the known signals remains at a high level. For the unknown radar waveform, it can be found that the discriminating ability of the P2 signal is improved significantly, and accuracy rate of it rises to 99%. In addition, the easy-confusing T2 signal has also been significantly improved, and its accuracy rate has also increased from 19% to 32%, the overall recognition rate has been improved.

D. STABILITY ANALYSIS OF FUSION MODEL

For the identification model of unknown signals, the significant difference from the previous known signal classification is the variability of the training set and the test set. According to the feature extraction scheme proposed in Section IV-A, two methods are used: swapping data set 2 and data set 3 and expanding data set 2 to complete the purpose of verifying the stability of the training set of the changing unknown signal.

First, the types of the unknown radar waveform have been changed. Meanwhile, the data set 1 of the training CNN remains unchanged, and it is still consisting of LFM, Costas, BPSK, and Frank. The data set 2 in the extraction of unknown features and the data set 3 in the transfer learning network test are swapped. That is to say, the training signals of the unknown signals are P1, P2, T1, and T2. And the test signals of the unknown signals are P3, P4, T3, and T4. The values of linear weight are obtained under the same simulation conditions in section IV-B. Then classification results of the decision fusion model, neuron mix model, and scheme 1 can be obtained after that. The results of decision fusion, neuron mixing, and scheme1 are shown in Figure 13.

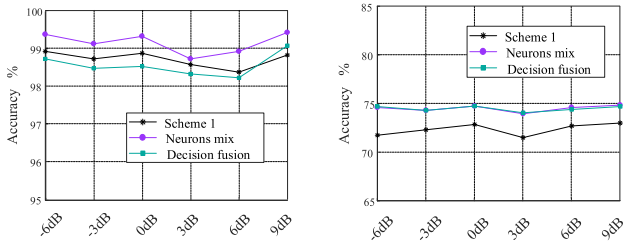

(a) Known signal accuracy (b) Unknown signal accuracy

FIGURE 13. Comparison of results of multiple classification models (change data set 3).

It can be seen from Figure 13 that, similar to the result in section IV-B, the decision fusion classification model and the neuron mix model still have promoted the recognition rate for unknown signals compared with scheme 1. The recognition results of the two models for unknown radar waveform are basically the same. And no matter the known radar waveform or unknown radar waveform, each SNR presents almost the same characteristic, which shows that this method has good stability. Compared with IV-B results, after changing the unknown radar signal style, the recognition accuracy of known signals remains at a high level.

No matter what kind of radar waveform samples are adopted, the decision fusion model based on transfer learning has improved significantly in unknown radar waveform recognition, and that further illustrates the neurons extracted from trained CNN and neurons extracted from non-trained CNN has differences. The difference is not related to the dataset of 2 and 3 always exists

Then, the type of unknown signal (extended dataset 2) is added to verify the stability of the model. For all the methods discussed above, data sets 1, 2, and 3 are all four signal waveforms. By comparing this simulation condition to the real battlefield environment, the known signal of dataset 1 is the signal waveform that we have mastered, while dataset 2 belongs to the unknown signal waveform relative to dataset 1, but it can also be considered as the signal that we want to distinguish from dataset 1 through prior knowledge. Through the previous data analysis, it can be seen that the decision fusion model proposed in this paper has a strong resolution ability for known signal waveform, and can achieve more than 99% recognition rate under the SNR ranging from-6dB to 9dB. For unknown signals, when the signals in data set 2 are not the same, although the trend is consistent, there are some differences in the recognition rate. Therefore, by adding signals in dataset 2, more unknown waveform features can be extracted to further improve the recognition ability of unknown signals. For data set 2, the other three signals BFSK-BPSK, LFM-BPSK and NCFM are added successively. Data set 1 and data set 3 remain unchanged as LFM, Costas, BPSK and Frank4 radar waveforms, and data set 3 is P1, P2, T1 and T2 signals. The same simulation conditions as VI-C-1 are adopted and the test results are shown in Figure 14.

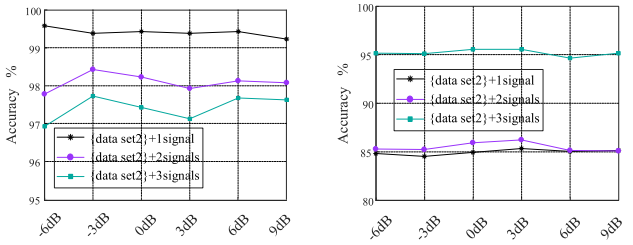

(a) Known signal accuracy (b) Unknown signal accuracy

FIGURE 14. Recognition rate of decision fusion classification model (extended data set 2).

After observation of Figure 14, It can be found the recognition accuracy of the known radar waveform decreases gradually as the number of signals increases. However, the recognition accuracy of the unknown radar waveform increases obviously as the number of signals increases.

It can be noticed that when the data set2 is added three kinds of radar waveforms, recognition accuracies of the known radar waveform and the unknown radar waveform both exceed 95%, maintaining a high recognition rate. Therefore, the selection of data set 2 can be adjusted according to the actual battlefield needs and the goals of the post-classification processing, which has guaranteed the accuracy of information acquisition.

V. CONCLUSION

An unknown radar signal recognition model based on transfer deep learning is proposed in this paper. Where, the reconstructed feature of signals is extracted and a linear weight decision fusion is used to improve the recognition accuracy. For the multiple feature image of the signal, a reconstruction feature extraction method based on transfer learning is proposed, and the neural value of the fully connected layer of the CNN is output to realize the reconstruction feature extraction after the signal is imaged. In order to realize the recognition of unknown radar waveforms, a multi-classifier system is used to analyze the changes of neurons, and linear weight decision fusion is used to realize the identification of unknown type.

Under the premise of knowing 4 kinds of signals, to identify different unknown new signals decision fusion method can greatly improve the recognition rate. In addition, changing the unknown signal types in the training and test set, the stability of the model always performances better; in addition, by increasing the training types of unknown signal samples, the model can improve the recognition accuracy of the unknown signal. And that can provide directions to the research of improving the recognition rate in the later period. But in the analysis of this paper, the recognition rate of unknown signals is generally below 85%, and there is a problem that it is difficult to extract a certain signal feature. The main work in the next step is mainly in two aspects: one is studying the change in the accuracy of network recognition in the condition of reducing the amount of unknown signal data in the training set; the other is to study feature extraction based on the determination of unknown signals. The optimization of the extractor can obtain the characteristics of the known signal to a greater extent and distinguish it from the characteristics of the unknown signal.

REFERENCES

[1] S. Q. Wang, J. Bai, X. Y. Huang, C. Y. Gao, and P. F. Wan, "Analysis of radar emitter signal sorting and recognition model structure," *Procedia Comput. Sci.*, vol. 154, pp. 500–503, Jan. 2019.
[2] J. D. Chen, *Research and Application of Radar Signal Recognition With Deep Learning Methods*. Chengdu, China: Univ. Electronic Science and Technology of China. 2019.
[3] K. Liu, Wang, J. G. Wang, J. F. Wu, "Intelligent recognition method based on interval grey association for unknown radar emitter," *Modern Defence Technol.*, vol. 41, no. 6, pp. 25–31, 2013.
[4] J. Guo and J. W. Chen, "Clustering approach for deinterleaving unknown radar signals," *Syst. Eng. Electron.*, vol. 28, no. 6, pp. 836–853, 2006.
[5] X. F. Wang, G. Y. Zhang, and J. Dai, "A new method of unknown radar signals sorting based on clustering," *Electron. Inf. Warfare Technol.*, vol. 27, no. 1, pp. 19–22, 2012.
[6] J. Chao, "An auto recognition method for in-pulse features of radar signal based on STFT," *Modern Inf. Technol.*, vol. 3, no. 1, pp. 50–53, 2019.
[7] W. Xu, J. Y. Jian, and M. Chen, "Intra-pulse modulation recognition of radar signal based on multi-dimensional features," *J. THz Sci. Electron. Inf. Technol.*, vol. 16, no. 1, pp. 81–86, 2018.
[8] J. Zhang, Y. Li, and J. Yin, "Modulation classification method for frequency modulation signals based on the time–frequency distribution and CNN," *IET Radar, Sonar Navigat.*, vol. 12, no. 2, pp. 244–249, Feb. 2018.
[9] Y. Zheng, Y. J. Shen, and Y. S. Zhou, "Radar signal modulation identification based on multilayer bidirectional LSTM," *J. Telemetry, Tracking Command*, vol. 40, no. 1, pp. 33–41, 2019.
[10] B. Jiang, Y. L. Mao, and J. F. Cao, "Application of probabilistic neural network model in modulation type recognition for radar signal," *Modern Electron. Technique*, vol. 41, no. 23, pp. 67–71, 2018.
[11] J. Yang and J. D. Yi, "Intra-pulse modulation recognition of radar signal based on three-dimensional features," *Telecommun. Eng.*, vol. 60, no. 3, pp. 279–283, 2020.
[12] F. Ying and W. Xing, "Radar signal recognition based on modified semi-supervised SVM algorithm," in *Proc. IEEE 2nd Adv. Inf. Technol., Electron. Autom. Control Conf. (IAEAC)*, Mar. 2017, pp. 2336–2340.
[13] G. H. Song, *Image Annotation Method Based on Transfer Learning and Deep Convolutional Feature*. Hangzhou, China: Zhejiang Univ., 2017.
[14] X. Q. Zhang, J. H. Chen, J. J. Zhuge, and L. J. Yu, "Deep learning based fast plant image recognition," *J. East China Univ. Sci. Technol. (Natural Sci. Edition).*, vol. 44, no. 6, pp. 887–895, 2018.
[15] Y. N. Lu, L. X. Lu, and D. F. Du, "Application of zero sample learning in image classification," *Electron. Technol. Softw. Eng.*, no. 12, p. 69, 2018.
[16] X. Li, *Research on Cross Domain Image Classification via Transfer Learning*. Xi'an, China: Xidian Univ., 2017.
[17] Z. L. Cai, Q. Wen, S. Z. Ye, and C. R. Jian, "Remote sensing image scene classification based on inception-V3," *Remote Sens. Land Resource*, vol. 32, no. 3, pp. 80–89, 2020.
[18] M. Han and X. Yang, "Transfer learning using improved Bayesian ARTMAP for remote sensing image classification," *Acta Electronica Sinica*, vol. 44, no. 9, pp. 2248–2253, 2016.
[19] C. Song, B. Wang, and J. T. Xu, "Research on tongue image classification methods based on deep transfer learning," *Comput. Eng. Sci.*, to be published.
[20] Y. X. Wang, *Power Data Mining Technology Based on Deep Learning and Transfer Learning*. angzhou, China: Zhejiang Univ., 2019.
[21] C. Chen, F. Shen, and Y. R. Qiang, "Enhanced least squares support vector machine-based transfer learning strategy for bearing fault diagnosis," (in Chinese), *Chin. J. Sci. Instrum.*, vol. 38, no. 1, pp. 33–40, Jan. 2017.
[22] S. Q. Kang, M. W. Hu, Y. J. Wang, J. B. Xie, and V. I. Mikulovich, "Fault diagnosis method of a rolling bearing under variable working conditions based on feature transfer learning," *Proc. CSEE*, vol. 39, no. 3, pp. 764–772, Feb. 2019.
[23] A. Kawalec and R. Owczarek, "Radar emitter recognition using intra pulse data," in *Proc. 15th Int. Conf. Microw., Radar Wireless Commun.*, Warsaw, Poland, vol. 2, May 2004, pp. 435–438.
[24] G. M. Wang, S. W. Chen, J. Huang, X. Qin, and J. J. Yuan, "Radar emitter sorting and recognition based on multi-synchrosqueezing transform," *Modern Radar.*, vol. 42, no. 3, pp. 49–56, 2020.
[25] S. Wei, Q. Qu, H. Su, M. Wang, J. Shi, and X. Hao, "Intra-pulse modulation radar signal recognition based on CLDN network," *IET Radar, Sonar Navigat.*, vol. 14, no. 6, pp. 803–810, Jun. 2020.
[26] G. Lan, B. Yoshua, and C. Aaron, *Deep Learning*, vol. 97. Cambridge, MA, USA: MIT Press, 2016.
[27] S. Jialin Pan and Q. Yang, "A survey on transfer learning," *IEEE Trans. Knowl. Data Eng.*, vol. 22, no. 10, pp. 1345–1359, Oct. 2010.
[28] F. Z. Zhuang, P. Luo, Q. He, and Z. Z. Shi, "Survey on transfer learning research," *J. Softw.*, vol. 26, no. 1, pp. 26–39, 2015.
[29] Y. Jason, C. Jeff, B. Yoshua, and L. Hod, "How transferable are features in deep neural networks," in *Proc. Adv. Neural Inf. Process. Syst. NIPS*, 2014, pp. 3320–3328.
[30] L. Gao, X. Zhang, J. Gao, and S. You, "Fusion image based radar signal feature extraction and modulation recognition," *IEEE Access*, vol. 7, pp. 13135–13148, 2019.
[31] G. M. Wang, S. Chen, J. Huang, and D. Huang, "Radar signal sorting and recognition based on transferred deep learning," *Comput. Sci. Appl.*, vol. 09, no. 09, pp. 1761–1778, 2019.
[32] Q. Guo, X. Yu, and G. Ruan, "LPI radar waveform recognition based on deep convolutional neural network transfer learning," *Symmetry*, vol. 11, no. 4, p. 540, Apr. 2019.
[33] X. Yan, Y. Jin, Y. Xu, and R. Li, "Wind turbine generator fault detection based on multi-layer neural network and random forest algorithm," in *Proc. IEEE Innov. Smart Grid Technol. Asia (ISGT Asia)*, May 2019, pp. 4132–4136.
[34] X. B. Liu, J. S. Liu, B. Liu, L. L. Qin, and T. Chen, "A novel algorithm of signal pre-sorting based on random forest," *Sci. Technol. Rev.*, vol. 37, no. 13, pp. 93–97, 2019.
[35] T. Lei, S. Y. Kuang, and L. Yang, "Radar emitter type identification algorithm based on deep learning," *Electron. Inf. Warfare Technol.*, vol. 34, no. 4, pp. 29–34, 2019.
[36] Z. Ma, Z. Huang, A. Lin, and G. Huang, "Emitter signal waveform classification based on autocorrelation and time-frequency analysis," *Electronics*, vol. 8, no. 12, p. 1419, Nov. 2019.

[37] J. Wen, J. Weng, C. Tong, C. Ren, and Z. Zhou, "Sparse signal recovery with minimization of 1-Norm minus 2-Norm," *IEEE Trans. Veh. Technol.*, vol. 68, no. 7, pp. 6847–6854, Jul. 2019.
[38] Z. Huang, Z. Ma, and G. Huang, "Radar waveform recognition based on multiple autocorrelation images," *IEEE Access*, vol. 7, pp. 98653–98668, 2019.
[39] S.-H. Kong, M. Kim, L. M. Hoang, and E. Kim, "Automatic LPI radar waveform recognition using CNN," *IEEE Access*, vol. 6, pp. 4207–4219, 2018.
[40] G. Q. Liu, X. Zhang, and Q. B. Lv, "The realization of smoothed pseudo wigner-ville distribution based on LabVIEW," *Appl. Mech. Mater.*, vols. 239–240, pp. 1493–1496, Dec. 2012.
[41] Z. Liu, Y. Shi, Y. Zeng, and Y. Gong, "Radar emitter signal detection with convolutional neural network," in *Proc. IEEE 11th Int. Conf. Adv. Infocomm Technol. (ICAIT)*, Oct. 2019, pp. 48–51.
[42] J. Z. Gao, *Detection of Weak Signal*. Beijing, China: Tsinghua Univ. Press, 2004, pp. 11–17.
[43] A. Krizhevsky, I. Sutskever, and G. E. Hinton, "ImageNet classification with deep convolutional neural networks," in *Proc. Adv. Neural Inf. Process. Systems.*, 2012, pp. 1097–1105.
[44] X. Guan, G. Liu, C. Huang, Q. Liu, C. Wu, Y. Jin, and Y. Li, "An object-based linear weight assignment fusion scheme to improve classification accuracy using landsat and MODIS data at the decision level," *IEEE Trans. Geosci. Remote Sens.*, vol. 55, no. 12, pp. 6989–7002, Dec. 2017.
[45] M. Kanmani and V. Narasimhan, "An optimal weighted averaging fusion strategy for thermal and visible images using dual tree discrete wavelet transform and self tunning particle swarm optimization," *Multimedia Tools Appl.*, vol. 76, no. 20, pp. 20989–21010, Oct. 2017.
[46] B. Khaleghi, A. Khamis, F. O. Karray, and S. N. Razavi, "Multi sensor data fusion: A review of the state-of-the-art," *Inf. Fusion.*, vol. 14, no. 1, pp. 28–44, 2013.
[47] H. Gholizadeh, M. J. V. Zoej, and B. Mojaradi, "A decision fusion approach for clustering of hyperspectral data using spectral unmixing methods," in *Proc. IEEE Aerosp. Conf.*, Mar. 2012, pp. 1–7.
[48] L. Breiman, "Random forests," *Machine Learn.*, vol. 45, no. 1, pp. 5–32, 2001.
[49] X. Zhou, P. Lu, Z. Zheng, D. Tolliver, and A. Keramati, "Accident prediction accuracy assessment for highway-rail grade crossings using random forest algorithm compared with decision tree," *Rel. Eng. Syst. Saf.*, vol. 200, Aug. 2020, Art. no. 106931.

ANNI LIN was born in Zhejiang, China, in 1991. She received the B.E. degree in computer science and technology from the Naval University of Engineering, Wuhan, Hubei, in 2014, where she is currently pursuing the M.E. degree in electronics and communication engineering. Her research interests include image processing, signal processing, and deep learning.

ZHIYUAN MA was born in Hubei, China, in 1982. He received the M.E. degree in electronic circuit and system from Central China Normal University, China, in 2007, where he is currently pursuing the Ph.D. degree in radio physics. He is currently an Assistant Professor with the Department of Electronic Technique, Naval University of Engineering, China. His research interest is intelligent signal processing.

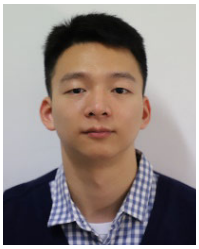

ZHI HUANG was born in Fujian, China, in 1994. He received the master's degree in circuits and systems from the Naval University of Engineering, Wuhan, Hubei, in 2019, where he is currently pursuing the Ph.D. degree in information and communication engineering. His research interests include emitter recognition, deep learning, and signal processing.

YAN XIA was born in Hubei, China, in 1988. He received the B.E. degree in electronic information engineering from Hubei University, Wuhan, Hubei, China, in 2012. He is currently pursuing the M.E. degree in electronics and communication engineering with the Naval University of Engineering, Wuhan. His research interests include electronic technology, signal processing, emitter recognition, and deep learning.

WENTING YU was born in Jiangxi, China, in 1994. She received the B.E. degree in electronic and information engineering from Nanchang Hangkong University, in 2015, where she is currently pursuing the master's degree in electronic and communication engineering. Her research interests include radiation-source signal recognition, transfer learning, and signal processing.